

Horizontal flow and capillarity-driven redistribution in porous media

F. Doster, O. Hönig, and R. Hilfer

Institut für Computerphysik, Universität Stuttgart, Pfaffenwaldring 27, 70569 Stuttgart, Germany

(Received 11 October 2011; published 18 July 2012)

A recent macroscopic mixture theory for two-phase immiscible displacement in porous media has introduced percolating and nonpercolating phases. Quasi-analytic solutions are computed and compared to the traditional theory. The solutions illustrate physical insights and effects due to spatiotemporal changes of nonpercolating phases, and they highlight the differences from traditional theory. Two initial and boundary value problems are solved in one spatial dimension. In the first problem a fluid is displaced by another fluid in a horizontal homogeneous porous medium. The displacing fluid is injected with a flow rate that keeps the saturation constant at the injection point. In the second problem a horizontal homogeneous porous medium is considered which is divided into two subdomains with different but constant initial saturations. Capillary forces lead to a redistribution of the fluids. Errors in the literature are reported and corrected.

DOI: [10.1103/PhysRevE.86.016317](https://doi.org/10.1103/PhysRevE.86.016317)

PACS number(s): 47.56.+r, 47.55.df, 47.55.dr

I. INTRODUCTION

Although numerous natural and technical processes involve two-phase flow in porous media, their theoretical description has remained a challenge for many decades [1] (see [2–5] as well as [6,7] for more recent historical remarks). Darcy’s law is commonly extended to two or more immiscible fluids using the concepts of relative permeability and capillary pressure [8–11].

The applicability of the traditional and commonly accepted generalized Darcy theory (subsequently called “traditional”) is limited to extremely slow displacement processes, so slow that the interfacial motion and momentum exchange between the two fluid phases are negligible. Because of these severe limitations its predictive power is limited to simple problems where hysteresis, dynamic effects (such as time-dependent capillary pressures or relative permeabilities), or varying residual saturations are not important. Alternative theories range from explicit hysteresis models [12–14] to modifications of the capillary pressure or relative permeabilities with additional unknowns [15–18]. Although it is well known that percolating and nonpercolating fluid parts show fundamentally different behavior [8,19–22], this fact is not reflected in the traditional theory. A macroscopic model which takes the difference between nonpercolating and percolating fluid parts explicitly into account was first proposed in Ref. [23] and further elaborated in subsequent publications [6,7,24–27]. This model no longer suffers from the restriction to extremely slow velocities because it allows for interfacial motion. In recent works numerical and analytical solutions of initial and boundary value problems of this theory have been computed [28–30].

In this paper similarity solutions are found for two idealized problems. These further enrich and explore the new theory. The first idealized problem considers co- and countercurrent flows in a semi-infinite porous medium. The medium is closed at infinity with a wall whose permeability can be changed from permeable to impermeable. The second problem concerns redistribution of the two immiscible fluids driven by capillary forces in an infinite horizontal medium. Methodically, both systems of coupled nonlinear partial differential equations including initial and boundary conditions admit similarity

solutions, which can be found by solving simpler ordinary differential or integro-differential equations.

In Sec. II of the paper a brief review of the model is given. In Secs. III and IV, simplifying assumptions are stated. These assumptions admit a quasi-analytical treatment of the system of coupled nonlinear partial differential equations for certain initial and boundary value problems. Two of them are presented in Sec. V. The first one resembles the McWhorter-Sunada problem [31] but accounts for percolating and nonpercolating fluid parts. Its solutions are discussed in Sec. VII and examples are given. The second is an adaptation of the redistribution problem of Philip [32] and is solved and discussed in Sec. VIII. Concluding remarks are given in Sec. IX.

II. DEFINITION OF THE MODEL**A. Balance laws and constitutive assumptions**

The basic idea of percolating and nonpercolating fluid phases was originally introduced in Refs. [23–25], and a closed mathematical model was formulated in Refs. [6,7,26]. Some numerical solutions have been obtained in Refs. [28,29]. In this section the model is restricted to one spatial dimension.

Percolating (=hydraulically connected) and nonpercolating (=hydraulically not connected, trapped) fluid parts are distinguished as separate phases. A mathematically precise definition of percolating and nonpercolating phases was given in Refs. [6] (p. 016307), [7] (p. 213), [26] (p. 121), and [27] (p. 142f) and is therefore not repeated here. Note that the definition is completely general. It applies also in cases where wetting films are present. Hence, a two-phase system is treated as a four-phase system. Following the notation of [7] the wetting fluid is named water and indexed with \mathbb{W} , while the nonwetting fluid is called oil and indexed with \mathbb{O} . The percolating water is identified with index $i = 1$, the nonpercolating water with $i = 2$, the percolating oil with $i = 3$, and the nonpercolating oil with $i = 4$. The index $i = 5$ represents the rock matrix. Volume conservation requires

$$S_1 + S_2 + S_3 + S_4 = 1, \quad (1)$$

where $S_i(x, t)$ is the saturation of phase i as function of position $x \in \mathbb{S} \subset \mathbb{R}$ and time $t \geq t_0$. From here on $t_0 = 0$ is assumed

without loss of generality. The one-dimensional sample region $\mathbb{S} \subset \mathbb{R}$ is an (infinite or finite) interval. The mass balance for fluid phase $i \in \{1, 2, 3, 4\}$ in a one-dimensional porous medium is expressed in differential form as

$$\frac{\partial(\phi S_i \varrho_i)}{\partial t} + \frac{\partial(\phi S_i \varrho_i v_i)}{\partial x} = M_i, \quad (2)$$

where $\varrho_i(x, t), \phi(x, t), v_i(x, t)$ are mass density, porosity, and velocity of phase i as functions of position $x \in \mathbb{S}$ and time $t \in \mathbb{R}_+$, and M_i is a source or sink term for the corresponding phase. For incompressible fluids and rigid homogeneous media one assumes

$$\phi(x, t) = \phi, \quad (3a)$$

$$\varrho_1(x, t) = \varrho_{\mathbb{W}}, \quad (3b)$$

$$\varrho_2(x, t) = \varrho_{\mathbb{W}}, \quad (3c)$$

$$\varrho_3(x, t) = \varrho_{\mathbb{O}}, \quad (3d)$$

$$\varrho_4(x, t) = \varrho_{\mathbb{O}} \quad (3e)$$

independent of x and t . Here $\varrho_{\mathbb{W}}, \varrho_{\mathbb{O}}$ are the densities of water and oil.

The source terms M_i in Eq. (2) allows one to model the mass exchange between percolating and nonpercolating phases through breakup and coalescence. They were assumed in Refs. [6,7,26] to be proportional to the rate $\partial S_{\mathbb{W}}/\partial t$ of saturation change as

$$M_1(S_{\mathbb{W}}, S_2, \partial_t S_{\mathbb{W}}) = -M_2 = \eta_2 \phi \varrho_{\mathbb{W}} \left(\frac{S_2 - S_2^*}{S_{\mathbb{W}}^* - S_{\mathbb{W}}} \right) \frac{\partial S_{\mathbb{W}}}{\partial t}, \quad (4a)$$

$$M_3(S_{\mathbb{W}}, S_4, \partial_t S_{\mathbb{W}}) = -M_4 = \eta_4 \phi \varrho_{\mathbb{O}} \left(\frac{S_4 - S_4^*}{S_{\mathbb{W}}^* - S_{\mathbb{W}}} \right) \frac{\partial S_{\mathbb{W}}}{\partial t}, \quad (4b)$$

where η_2, η_4 are constants and the short-hand $\partial_t = \partial/\partial t$ was used. The factor in brackets postulates that the mass exchange between percolating and nonpercolating phases is proportional to the amount of nonpercolating phase present. The parameters $S_{\mathbb{W}}^*, S_2^*$, and S_4^* are defined by

$$S_{\mathbb{W}}^*(\partial_t S_{\mathbb{W}}) = (1 - S_{\mathbb{O} \text{ im}}) \Theta(\partial_t S_{\mathbb{W}}) + S_{\mathbb{W} \text{ dr}} [1 - \Theta(\partial_t S_{\mathbb{W}})], \quad (5a)$$

$$S_2^*(\partial_t S_{\mathbb{W}}) = S_{\mathbb{W} \text{ dr}} [1 - \Theta(\partial_t S_{\mathbb{W}})], \quad (5b)$$

$$S_4^*(\partial_t S_{\mathbb{W}}) = S_{\mathbb{O} \text{ im}} \Theta(\partial_t S_{\mathbb{W}}), \quad (5c)$$

where $S_{\mathbb{W} \text{ dr}}, S_{\mathbb{O} \text{ im}}$ are limiting saturations for S_2, S_4 and $\Theta(x)$ denotes the Heaviside unit step function.

The momentum balance is written for phase $i \in \{1, 2, 3, 4\}$ as

$$\phi S_i \varrho_i \frac{D^i}{Dt} v_i - \phi S_i \frac{\partial \Sigma_i}{\partial x} - \phi S_i F_i = m_i - v_i M_i, \quad (6)$$

where $D^i/Dt = \partial/\partial t + v_i \partial/\partial x$ denotes the material derivative for phase i , Σ_i the stress tensor in the i th phase, F_i the body force per unit volume acting on the i th phase and m_i denotes the momentum transfer into phase i from all the other phases. The material derivatives are neglected here, i.e.,

$$\phi S_i \varrho_i \frac{D^i v_i}{Dt} = 0, \quad (7)$$

because realistic subsurface flows have small Reynolds numbers [33]. Note, however, that interfacial motion takes place. The stress tensors for the four phases are specified as

$$\Sigma_1(P_1) = -P_1, \quad (8a)$$

$$\Sigma_2(P_3, S_2) = -P_3 + \gamma P_2^* S_2^{\gamma-1}, \quad (8b)$$

$$\Sigma_3(P_3) = -P_3, \quad (8c)$$

$$\Sigma_4(P_1, S_4) = -P_1 + \delta P_4^* S_4^{\delta-1}, \quad (8d)$$

where $P_1(x, t)$ and $P_3(x, t)$ are the fluid pressures in the percolating phases, and the constants P_2^*, P_4^* and exponents γ, δ account for surface tension effects.

The momentum transfer m_i in Eq. (6) is assumed to be given by linear viscous drag. More specifically, they are assumed linear in the velocity differences

$$m_1(v_1, v_3, v_4) = R_{13}(v_3 - v_1) + R_{14}(v_4 - v_1) - R_{15}v_1, \quad (9a)$$

$$m_2(v_2, v_3, v_4) = R_{23}(v_3 - v_2) + R_{24}(v_4 - v_2) - R_{25}v_2, \quad (9b)$$

$$m_3(v_1, v_2, v_3) = R_{31}(v_1 - v_3) + R_{32}(v_2 - v_3) - R_{35}v_3, \quad (9c)$$

$$m_4(v_1, v_2, v_4) = R_{41}(v_1 - v_4) + R_{42}(v_2 - v_4) - R_{45}v_4, \quad (9d)$$

where the resistance coefficients R_{ij} are assumed to be constitutive parameters. The last terms on the right-hand side represent viscous drag between the fluid phases and the wall, whose velocity is $v_5 = 0$. The resistance coefficients $R_{12} = 0$ and $R_{34} = 0$ were assumed to vanish, because there is no common interface and hence no direct viscous drag between these phase pairs.

The body forces are given by gravity and capillarity. Capillary body forces for the nonpercolating phases are necessary in a macroscopic theory, because these fluid parts are acted upon by gravity but neither sink nor rise in a porous medium. The capillary body forces were specified in Refs. [6,7,26] as

$$F_1 = \varrho_1 g \sin \vartheta, \quad (10a)$$

$$F_2(S_1, \partial_x S_1) = \varrho_2 g \sin \vartheta + \Pi_a \frac{\partial S_1^{-\alpha}}{\partial x}, \quad (10b)$$

$$F_3 = \varrho_3 g \sin \vartheta, \quad (10c)$$

$$F_4(S_3, \partial_x S_3) = \varrho_4 g \sin \vartheta + \Pi_b \frac{\partial S_3^{-\beta}}{\partial x}, \quad (10d)$$

with constitutive parameters Π_a, Π_b and exponents $\alpha, \beta > 0$. The angle $0 \leq \vartheta \leq \pi/2$ is the angle between the direction of the column and the direction of gravity. For $\vartheta = 0$ the column is oriented perpendicular to gravity, while $\vartheta = \pi/2$ corresponds to alignment. For more details on the physical motivation of the constitutive assumptions we refer the reader to the original publications [6,7,26,27].

B. Reformulation of the model

The balance laws (1), (2), and (6) are rearranged in terms of volume flux densities. Inserting Eq. (7) into Eq. (6) it becomes linear in the velocities v_i . Its right-hand side can be written as

$$\begin{pmatrix} m_1 - M_1 v_1 \\ m_2 + M_1 v_2 \\ m_3 - M_3 v_3 \\ m_4 + M_3 v_4 \end{pmatrix} = -\tilde{R} \begin{pmatrix} v_1 \\ v_2 \\ v_3 \\ v_4 \end{pmatrix}, \quad (11)$$

where the components of the generalized resistance matrix \tilde{R} are

$$\tilde{R}(S_{\mathbb{W}}, S_2, S_4, \partial_t S_{\mathbb{W}}) := \begin{pmatrix} R_{11} & 0 & -R_{13} & -R_{14} \\ 0 & R_{22} & -R_{23} & -R_{24} \\ -R_{31} & -R_{32} & R_{33} & 0 \\ -R_{41} & -R_{42} & 0 & R_{44} \end{pmatrix}, \quad (12)$$

and the short-hand notation

$$R_{11}(S_{\mathbb{W}}, S_2, \partial_t S_{\mathbb{W}}) := R_{15} + R_{13} + R_{14} + M_1, \quad (13a)$$

$$R_{22}(S_{\mathbb{W}}, S_2, \partial_t S_{\mathbb{W}}) := R_{25} + R_{23} + R_{24} - M_1, \quad (13b)$$

$$R_{33}(S_{\mathbb{W}}, S_4, \partial_t S_{\mathbb{W}}) := R_{35} + R_{31} + R_{32} + M_3, \quad (13c)$$

$$R_{44}(S_{\mathbb{W}}, S_4, \partial_t S_{\mathbb{W}}) := R_{45} + R_{41} + R_{42} - M_3 \quad (13d)$$

was used. To obtain expressions for the volume flux densities Q_i , Eq. (11) is inserted into Eq. (6). The resulting set of equations is solved for the velocities and multiplied with the corresponding phase volume fractions ϕS_i , $i \in \{1, 2, 3, 4\}$. As a result one finds

$$\begin{pmatrix} Q_1 \\ Q_2 \\ Q_3 \\ Q_4 \end{pmatrix} := \begin{pmatrix} \phi S_1 v_1 \\ \phi S_2 v_2 \\ \phi S_3 v_3 \\ \phi S_4 v_4 \end{pmatrix} = \Lambda \begin{pmatrix} \partial_x \Sigma_1 + F_1 \\ \partial_x \Sigma_2 + F_2 \\ \partial_x \Sigma_3 + F_3 \\ \partial_x \Sigma_4 + F_4 \end{pmatrix}, \quad (14)$$

where the mobility matrix Λ has been introduced. The components of Λ are given by

$$\lambda_{ij}(S_{\mathbb{W}}, S_2, S_4, \partial_t S_{\mathbb{W}}) := \phi^2 S_i S_j [\tilde{R}^{-1}]_{ij} \quad (15)$$

in terms of the inverse of \tilde{R} . The primary variables are $S_{\mathbb{W}}, S_2$, and S_4 . The mass balances (2) are combined linearly and volume conservation (1) is applied to obtain

$$\phi \frac{\partial S_{\mathbb{W}}}{\partial t} + \frac{\partial Q_{\mathbb{W}}}{\partial x} = 0, \quad (16a)$$

$$\phi \frac{\partial S_2}{\partial t} + \frac{\partial Q_2}{\partial x} = -\frac{M_1}{\varrho_{\mathbb{W}}}, \quad (16b)$$

$$\phi \frac{\partial S_4}{\partial t} + \frac{\partial Q_4}{\partial x} = -\frac{M_3}{\varrho_{\mathbb{O}}}, \quad (16c)$$

$$\frac{\partial}{\partial x} (Q_{\mathbb{W}} + Q_{\mathbb{O}}) = 0, \quad (16d)$$

where $Q_{\mathbb{W}} = Q_1 + Q_2$ and $Q_{\mathbb{O}} = Q_3 + Q_4$.

III. SIMPLIFYING ASSUMPTIONS

A. Immobility of nonpercolating fluids

As a first approximation it is assumed that the nonpercolating phases $i = 2, 4$ are immobile. This can be ensured by assuming that

$$R_{25} \gg R_{ij}, \quad (17a)$$

$$R_{45} \gg R_{ij} \quad (17b)$$

for all pairs (i, j) with $(i, j) \in \{1, 2, 3, 4\} \times \{1, 2, 3, 4, 5\}$ and $(i, j) \neq (2, 5)$ and $(i, j) \neq (4, 5)$. It will also be assumed that

$$R_{25} \gg M_1, \quad (18a)$$

$$R_{45} \gg M_3 \quad (18b)$$

holds. The approximation may be justified physically by the observation that the motion of contact lines on the internal surface requires that capillary forces be overcome, and this creates additional resistance that is much higher than the viscous drag.

In the limit $R_{25} \rightarrow \infty$, $R_{45} \rightarrow \infty$ only the components $\lambda_{11}, \lambda_{13}, \lambda_{31}, \lambda_{33}$ of the mobility matrix Λ differ from zero. Hence, the volume fluxes are approximated as

$$Q_{\mathbb{W}} = \lambda_{11}(\partial_x \Sigma_1 + F_1) + \lambda_{13}(\partial_x \Sigma_3 + F_3), \quad (19a)$$

$$Q_{\mathbb{O}} = \lambda_{31}(\partial_x \Sigma_1 + F_1) + \lambda_{33}(\partial_x \Sigma_3 + F_3), \quad (19b)$$

$$Q_2 = 0, \quad (19c)$$

$$Q_4 = 0, \quad (19d)$$

where the nonzero components of the mobility matrix are explicitly given by

$$\lambda_{11}(S_{\mathbb{W}}, S_2, S_4, \partial_t S_{\mathbb{W}}) = \phi^2 \frac{R_{33}}{R_{13}^2 + R_{11}R_{33}} S_1^2, \quad (20a)$$

$$\lambda_{13}(S_{\mathbb{W}}, S_2, S_4, \partial_t S_{\mathbb{W}}) = \phi^2 \frac{R_{13}}{R_{13}^2 + R_{11}R_{33}} S_1 S_3 = \lambda_{31}, \quad (20b)$$

$$\lambda_{33}(S_{\mathbb{W}}, S_2, S_4, \partial_t S_{\mathbb{W}}) = \phi^2 \frac{R_{11}}{R_{13}^2 + R_{11}R_{33}} S_3^2 \quad (20c)$$

in terms of the saturations

$$S_1(x, t) = S_{\mathbb{W}}(x, t) - S_2(x, t), \quad (21a)$$

$$S_3(x, t) = 1 - S_{\mathbb{W}}(x, t) - S_4(x, t). \quad (21b)$$

In Eq. (20) Onsager reciprocity $R_{31} = R_{13}$ is assumed to hold.

B. Viscous domination

When estimating orders of magnitudes in realistic experiments [28,29], one finds that the resistance coefficients R_{ij} are typically of order $10^8 \text{ kg m}^{-3} \text{ s}^{-1}$, while the momentum transfer due to mass exchange is only of order $10^3 \text{ kg m}^{-3} \text{ s}^{-1}$. Therefore, it is assumed that the viscous drag dominates the momentum transfer, so that

$$R_{15} \gg M_1 \quad \text{or} \quad R_{13} \gg M_1, \quad (22a)$$

$$R_{35} \gg M_3 \quad \text{or} \quad R_{13} \gg M_3 \quad (22b)$$

holds true. Then the resistance matrix

$$\tilde{R}(S_{\mathbb{W}}, S_2, S_4, \partial_t S_{\mathbb{W}}) = \tilde{R} \quad (23)$$

becomes a constant parameter matrix. Note that for $S_{\mathbb{W}} \rightarrow S_{\mathbb{W}}^*$ or $\partial_t S_{\mathbb{W}} \rightarrow \infty$, the assumption breaks down. This case is avoided here by assuming that the saturations $S_{\mathbb{W}}^*$ and $S_{\mathbb{W}}$ are usually not known with a precision better than 10^{-4} . Therefore, $|S_{\mathbb{W}}^* - S_{\mathbb{W}}| > 10^{-4}$ is enforced throughout. It is also assumed that the rate of saturation change in typical experiments is very slow and obeys $\partial_t S_{\mathbb{W}} < 1 \text{ s}^{-1}$.

C. Self-consistent closure condition

The system of nonlinear partial differential equations is closed self-consistently. The most general form of self-consistent closure was given in Refs. [28,29]. Here, a simplification is employed. Guided by the residual decoupling

approximation from [6,7] the relation

$$\frac{\partial P_3}{\partial x} = \frac{\partial P_1}{\partial x} + \frac{1}{2} \frac{\partial}{\partial x} (\Pi_a S_1^{-\alpha} - \Pi_b S_3^{-\beta} + \gamma P_2^* S_2^{\gamma-1} - \delta P_4^* S_4^{\delta-1}) \quad (24)$$

suffices to recover the traditional capillary pressure concept for sufficiently slow displacement processes from the generalized theory. The difference between the phase pressures of the percolating phases

$$P_c := P_3 - P_1 \quad (25)$$

is identified as the macroscopic capillary pressure P_c . Integrating Eq. (24) yields [6,7,26]

$$P_c(S_1, S_2, S_3, S_4) = \frac{1}{2} (\Pi_a S_1^{-\alpha} - \Pi_b S_3^{-\beta} + \gamma P_2^* S_2^{\gamma-1} - \delta P_4^* S_4^{\delta-1}) + C, \quad (26)$$

where the integration constant C is determined experimentally together with the parameters $\Pi_a, \Pi_b, P_2^*, P_4^*$ and the exponents $\alpha, \beta, \gamma, \delta$. Note that the number of parameters is less than in the traditional theory [see Eq. (12) in Ref. [7]]. For realistic values and experimental determination of these parameters see Sec. VII C below.

IV. MODEL REDUCTION AND FRACTIONAL MOBILITY FUNCTIONS

To obtain fractional flow and mobility functions, the approximations (17), (18), (22), and (26) are inserted into Eqs. (16). Equation (16d) implies that the total flux

$$Q(t) = Q_{\mathbb{W}}(x, t) + Q_{\mathbb{O}}(x, t) \quad (27)$$

is constant in the whole domain and depends only on time. By inserting Eqs. (8) and (10) into Eq. (19) and then inserting the result and Eq. (24) into Eq. (27), one finds

$$\frac{\partial P_1}{\partial x} = -\frac{1}{\lambda_{\mathbb{W}} + \lambda_{\mathbb{O}}} \left(Q(t) - \lambda_{\mathbb{W}} F_1 - \lambda_{\mathbb{O}} F_3 - \lambda_{\mathbb{O}} \frac{\partial P_c}{\partial x} \right) \quad (28)$$

for the pressure gradient of the percolating water. The mobilities of water and oil

$$\lambda_{\mathbb{W}}(S_{\mathbb{W}}, S_2, S_4) = \lambda_{11} + \lambda_{13}, \quad (29a)$$

$$\lambda_{\mathbb{O}}(S_{\mathbb{W}}, S_2, S_4) = \lambda_{33} + \lambda_{13} \quad (29b)$$

are introduced analogously to the traditional theory [3,10]. The fractional flow function $f_{\mathbb{W}}$ and the fractional mobility λ are defined as

$$f_{\mathbb{W}}(S_{\mathbb{W}}, S_2, S_4) = \frac{\lambda_{\mathbb{W}}}{\lambda_{\mathbb{W}} + \lambda_{\mathbb{O}}}, \quad (30a)$$

$$\lambda(S_{\mathbb{W}}, S_2, S_4) = \frac{\lambda_{11}\lambda_{33} - \lambda_{13}^2}{\lambda_{\mathbb{W}} + \lambda_{\mathbb{O}}}. \quad (30b)$$

Inserting Eqs. (8), (10), (25), (28), and (30) into Eq. (19) yields

$$Q_{\mathbb{W}} = f_{\mathbb{W}} Q(t) + \lambda(F_1 - F_3) + \lambda \frac{\partial P_c}{\partial x} \quad (31)$$

for the water flux. By inserting this into Eq. (16) a set of three coupled nonlinear partial differential equations

$$\phi \frac{\partial S_{\mathbb{W}}}{\partial t} + Q(t) \frac{\partial f_{\mathbb{W}}}{\partial x} + \frac{\partial}{\partial x} [\lambda(F_1 - F_3)] + \frac{\partial}{\partial x} \left(\lambda \frac{\partial P_c}{\partial x} \right) = 0, \quad (32a)$$

$$\phi \frac{\partial S_2}{\partial t} + \frac{M_1}{\varrho_{\mathbb{W}}} = 0, \quad (32b)$$

$$\phi \frac{\partial S_4}{\partial t} + \frac{M_3}{\varrho_{\mathbb{O}}} = 0 \quad (32c)$$

for the saturations $S_{\mathbb{W}}, S_2, S_4$ is obtained. If the flux $Q(t)$ is imposed externally, it is not necessary to solve the elliptic equation (28) for the pressure. The problem is then reduced to solving Eq. (32) for $S_{\mathbb{W}}, S_2, S_4$ subject to suitable initial and boundary conditions.

To avoid overcrowding the notation the index \mathbb{W} of the water saturation $S_{\mathbb{W}}$ is omitted in subsequent sections. From now on, S represents the water saturation instead of $S_{\mathbb{W}}$.

V. INITIAL AND BOUNDARY VALUES

Two initial and boundary value problems for Eqs. (32) are discussed here. The first problem searches for solutions with similarity variable x/\sqrt{t} in the co- and countercurrent displacement of a nonwetting fluid through a wetting fluid. The second problem considers capillarity-driven horizontal redistribution. For the traditional theory the first problem was discussed by McWhorter and Sunada in Ref. [31] and the second problem was discussed by Philip in Ref. [32].

A. Diffusive similarity solutions with decreasing flux [31]

Consider a one dimensional semi-infinite sample $\mathbb{S} = (0, \infty)$ which is mounted perpendicularly to gravity ($\vartheta = 0$). The medium has a wall of variable permeability at $x = \infty$. It is flooded from left to right with the wetting fluid. Diffusive similarity requires that the flux $Q_{\mathbb{W}}(0, t)$ at $x = 0$ has to decay as $1/\sqrt{t}$. The boundary conditions are

$$Q_{\mathbb{W}}(0, t) = \frac{A}{\sqrt{t}}, \quad (33a)$$

$$S(\infty, t) = S_r, \quad (33b)$$

$$S_i(\infty, t) = S_{ir} \quad (33c)$$

for all $t > 0$ and $i = 2, 4$. The parameter A has units $\text{ms}^{-1/2}$. Although the flux in Eq. (33a) diverges for $t \rightarrow 0$, it remains integrable, so that these boundary conditions can in principle be approximated in an experiment. It will be seen below that Eq. (33a) at $x = 0$ leads to constant $S_{\ell} = S(0, t)$ at $x = 0$. This allows one to replace A with S_{ℓ} in numerical computations. The initial saturations are specified with $i = 2, 4$ as

$$S_{\mathbb{W}0}(x) = S(x, 0) = S_r, \quad (34a)$$

$$S_{i0}(x) = S_i(x, 0) = S_{ir} \quad (34b)$$

on the semi-infinite domain $(0, \infty)$.

B. Capillarity-driven horizontal redistribution [32]

In the capillarity-driven horizontal redistribution problem one considers an infinite sample $\mathbb{S} = \mathbb{R}$ perpendicular to gravity ($\vartheta = 0$). The sample is closed at both ends. This means that the total volume flux

$$Q(t) = 0 \quad (35)$$

vanishes for all times $t \geq 0$. The initial saturation profiles are discontinuous at $x = 0$, so that

$$S_{\mathbb{W}0}(x) = S(x, 0) = S_\ell + (S_r - S_\ell)\Theta(x), \quad (36a)$$

$$S_{i0}(x) = S_i(x, 0) = S_{i\ell} + (S_{ir} - S_{i\ell})\Theta(x), \quad (36b)$$

where $i = 2, 4$, $-\infty < x < \infty$, and $\Theta(x)$ is the Heaviside step function. The boundary conditions are

$$S(-\infty, t) = S_\ell, \quad (37a)$$

$$S_i(-\infty, t) = S_{i\ell}, \quad (37b)$$

$$S(\infty, t) = S_r, \quad (37c)$$

$$S_i(\infty, t) = S_{ir} \quad (37d)$$

for all $t > 0$ and $i = 2, 4$.

VI. FRACTIONAL FLOW FORMULATION

Both problems defined in Sec. V concern horizontal media without gravity. In this case $\vartheta = 0$, and the body forces

$$F_1 = 0, \quad (38a)$$

$$F_3 = 0 \quad (38b)$$

are absent. Inserting Eqs. (38) and the mass exchange terms from Eq. (4) into Eqs. (32) one finds

$$\phi \frac{\partial S}{\partial t} + \frac{\partial}{\partial x} \left[Q(t) f_{\mathbb{W}}(S, S_2, S_4) + \lambda(S, S_2, S_4) \frac{\partial}{\partial x} P_c(S, S_2, S_4) \right] = 0, \quad (39a)$$

$$\frac{\partial S_2}{\partial t} = -\eta_2 \left(\frac{S_2 - S_2^*}{S_{\mathbb{W}}^* - S} \right) \frac{\partial S}{\partial t}, \quad (39b)$$

$$\frac{\partial S_4}{\partial t} = -\eta_4 \left(\frac{S_4 - S_4^*}{S_{\mathbb{W}}^* - S} \right) \frac{\partial S}{\partial t}. \quad (39c)$$

Equations (39b) and (39c) have the solutions [7]

$$S_2(x, t) = S_2^* + (S_{20}(x) - S_2^*) \left(\frac{S_{\mathbb{W}}^* - S(x, t)}{S_{\mathbb{W}}^* - S_{\mathbb{W}0}(x)} \right)^{\eta_2}, \quad (40a)$$

$$S_4(x, t) = S_4^* + (S_{40}(x) - S_4^*) \left(\frac{S(x, t) - S_{\mathbb{W}}^*}{S_{\mathbb{W}0}(x) - S_{\mathbb{W}}^*} \right)^{\eta_4}, \quad (40b)$$

where the initial saturations are given by Eqs. (34) or (36). The limiting saturations $S_{\mathbb{W}}^*$, S_2^* , S_4^* are given by Eqs. (5). For imbibition processes [i.e., for $\partial_t S(x, t) > 0$ for $t \geq 0$]

$$S_{\mathbb{W}}^*(x, t) = 1 - S_{\text{O im}}, \quad (41a)$$

$$S_2^*(x, t) = 0, \quad (41b)$$

$$S_4^*(x, t) = S_{\text{O im}} \quad (41c)$$

holds, while

$$S_{\mathbb{W}}^*(x, t) = S_{\mathbb{W} \text{ dr}}, \quad (42a)$$

$$S_2^*(x, t) = S_{\mathbb{W} \text{ dr}}, \quad (42b)$$

$$S_4^*(x, t) = 0 \quad (42c)$$

holds for drainage processes [i.e., for $\partial_t S(x, t) < 0$ for $t \geq 0$].

The fractional flow formulation

$$\phi \frac{\partial S}{\partial t} + \frac{\partial}{\partial x} \left(Q(t) f_{\mathbb{W}}(S) - D(S) \frac{\partial S}{\partial x} \right) = 0 \quad (43)$$

is obtained by inserting Eq. (40) into Eq. (39a). The fractional flow function $f_{\mathbb{W}}(S)$ and the so called ‘‘capillary diffusion coefficient’’ $D(S)$ are defined as

$$f_{\mathbb{W}}(S) = f_{\mathbb{W}}(S, S_2, S_4), \quad (44a)$$

$$D(S) = -\lambda(S, S_2, S_4) \frac{d}{dS} P_c(S, S_2, S_4), \quad (44b)$$

where $S_2 = S_2(S; S_{\mathbb{W}0}, S_{20})$ and $S_4 = S_4(S; S_{\mathbb{W}0}, S_{40})$. The initial conditions may introduce an explicit x dependence into $f_{\mathbb{W}}$ and D .

Contrary to the traditional theory, the parameter functions $P_c(S; S_{\mathbb{W}0}, S_{20}, S_{40})$ as well as $f_{\mathbb{W}}(S; S_{\mathbb{W}0}, S_{20}, S_{40})$ and $\lambda(S; S_{\mathbb{W}0}, S_{20}, S_{40})$ of the present theory depend not only on the saturation but also on the type of process through the initial conditions $S_{\mathbb{W}0}, S_{20}, S_{40}$. Figures 1 and 2 illustrate these functions for four typical processes, namely, primary and secondary drainage and imbibition. The initial saturations for these four processes are listed in Table I.

A displacement process is named *primary imbibition* if water invades a completely oil filled porous medium. It is named *primary drainage* if oil invades a completely water filled porous medium. A displacement process is named a *secondary drainage* if the water is displaced starting from the maximum saturation $S = 1 - S_{\text{O im}}$ of a preceding primary imbibition. It is named a *secondary imbibition* analogously.

Figure 1 shows four typical $P_c(S)$ functions for primary and secondary drainage and imbibition computed from

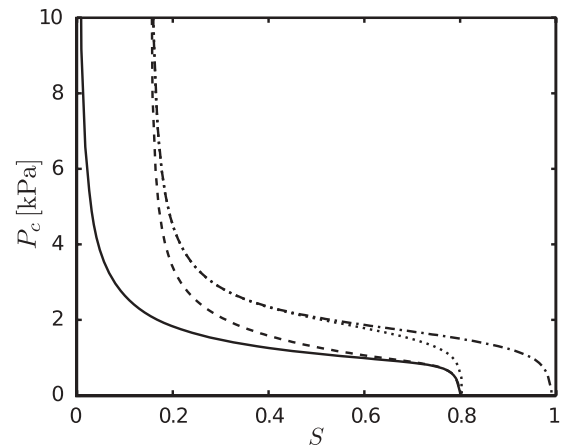


FIG. 1. Typical capillary pressure vs water saturation relation $P_c(S; S_{\mathbb{W}0}, S_{20}, S_{40})$ for primary imbibition (solid), secondary imbibition (dashed), primary drainage (dash-dotted), and secondary drainage (dotted). The corresponding initial saturations $S_{\mathbb{W}0}, S_{20}, S_{40}$ are listed in Table I, while the parameter values are listed in Table II.

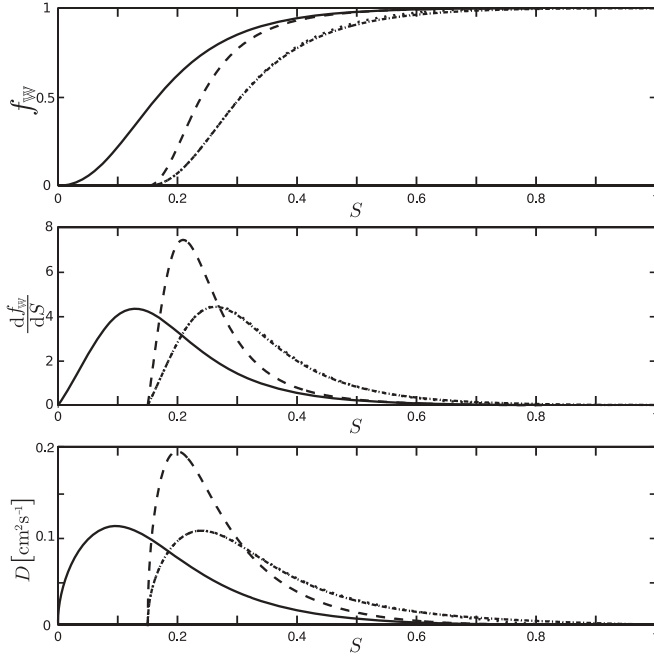


FIG. 2. Parameter functions for characteristic processes. From top to bottom the fractional flow function $f_{\mathbb{W}}(S)$, its derivative $df_{\mathbb{W}}(S)/dS$ and the macroscopic capillary diffusion coefficient $D(S)$ are shown. Solid curves show primary imbibition functions, dashed curves show secondary imbibition functions, dash-dotted curves show primary drainage, and dotted curves show secondary drainage processes.

Eqs. (26) and (40). They correspond to the initial saturations $S_{\mathbb{W}0}, S_{20}, S_{40}$ listed in Table I. The capillary pressure is higher for drainage processes than for imbibition processes. The primary curves enclose the secondary curves. The secondary curves form the main hysteresis loop ranging from $S = S_{\mathbb{W} \text{ dr}}$ to $S = S_{\odot \text{ im}}$. For parameter values see Table II.

Figure 2 illustrates the fractional flow function $f_{\mathbb{W}}(S)$, its derivative $df_{\mathbb{W}}/dS$, and the macroscopic capillary coefficient $D(S)$ for the processes shown in Fig. 1. Note that the primary and secondary drainage curves almost coincide for $S \in [S_{\mathbb{W} \text{ dr}}, 1 - S_{\odot \text{ im}}]$ for all three functions. The reason for this coincidence is that $R_{33}/R_{11} \approx 20$ (see Table II).

The fractional flow functions $f_{\mathbb{W}}(S)$ give the fraction of the advective water flux to total advective flux at saturation S . The fraction is higher for imbibition processes than for drainage processes and the primary curves enclose the secondary curves

TABLE I. Initial saturations $S_{\mathbb{W}0}, S_{20}, S_{40}$ for primary and secondary imbibition as well as primary and secondary drainage processes.

	Primary imbibition	Secondary imbibition	Primary drainage	Secondary drainage
$S_{\mathbb{W}0}$	0	$S_{\mathbb{W} \text{ dr}}$	1	$1 - S_{\odot \text{ im}}$
S_{20}	0	$S_{\mathbb{W} \text{ dr}}$	0	0
S_{40}	0	0	0	$S_{\odot \text{ im}}$

TABLE II. Values of the parameters taken from [7]. The viscous resistances correspond to viscosities $\mu_{\mathbb{W}} = 0.001 \text{ kg m}^{-1} \text{ s}^{-1}$ and $\mu_{\odot} = 0.02 \text{ kg m}^{-1} \text{ s}^{-1}$ and a permeability of $k = 1.0 \times 10^{-11} \text{ m}^2$.

Water			Oil		
Parameter	Value	Units	Parameter	Value	Units
$Q_{\mathbb{W}}$	1000	kg m^{-3}	Q_{\odot}	800	kg m^{-3}
η_2	4		η_4	3	
$S_{\mathbb{W} \text{ dr}}$	0.15		$S_{\odot \text{ im}}$	0.19	
Π_a	1620	Pa	Π_b	25	Pa
α	0.52		β	0.90	
P_2^*	2500	Pa	P_4^*	400	Pa
γ	1.5		δ	3.5	
R_{11}	1.16	$10^6 \text{ kg m}^{-3} \text{ s}^{-1}$	R_{33}	2.31	$10^7 \text{ kg m}^{-3} \text{ s}^{-1}$
R_{13}	0	$\text{kg m}^{-3} \text{ s}^{-1}$	R_{31}	0	$\text{kg m}^{-3} \text{ s}^{-1}$

which form the main hysteresis loop ranging from $S = S_{\mathbb{W} \text{ dr}}$ to $S = 1 - S_{\odot \text{ im}}$.

The derivative $df_{\mathbb{W}}/dS$ of the fractional flow functions is the velocity of advective waves in terms of the total flux Q/ϕ in the porous medium. The maximum velocity is higher for the secondary imbibition than for the primary imbibition and the saturation at the maximum velocity is higher for drainage than for imbibition.

The nonlinear diffusion coefficient $D(S)$ shows a single maximum for all processes. The maxima of the two drainage processes almost coincide in terms of magnitude and saturation. For the secondary imbibition, the maximal diffusion and its saturation are ceteris paribus significantly larger than those for the primary imbibition.

VII. DIFFUSIVE SIMILARITY SOLUTIONS WITH DECREASING FLUX [31]

A. General solution

Consider Eq. (43) with initial conditions (34) and boundary conditions (33). Following McWhorter and Sunada [31,34,35] a similarity solution

$$S(x,t) = S\left(\frac{x}{\sqrt{t}}\right) = S(\eta) \quad (45)$$

with similarity variable $\eta = x/\sqrt{t}$ will be searched for [36]. Inserting Eq. (45) into Eq. (43) shows that an ordinary differential equation for $S(\eta)$ is obtained if $Q(t) \sim 1/\sqrt{t}$. Combining this observation with Eqs. (27) and (33a) suggests that we can define a proportionality factor r by

$$Q(t) = r Q_{\mathbb{W}}(0,t) = \frac{rA}{\sqrt{t}}. \quad (46)$$

The coefficient r must obey $0 \leq r \leq 1$. It is bounded by $r \leq 1$ because of volume conservation, and $r \geq 0$ because the wetting phase is injected from left to right. r may be viewed as a normalized ‘‘permeability at infinity.’’ $r = 0$ corresponds to an impermeable wall at the right boundary. $r = 1$ represents free outflow conditions at $x = \infty$, and $Q_{\odot}(0,t) = 0$ at $x = 0$. Therefore the flow of water and oil is cocurrent for $r = 1$ and countercurrent for $r = 0$. The total flux is constant [see Eq. (27)] in the whole medium because both fluids are incompressible.

Equation (43) is now rewritten as

$$\phi \frac{\partial S}{\partial t} + Q_{\mathbb{W}}(0,t) [1 - rf_{\mathbb{W}}(S_r)] \frac{\partial F}{\partial x} = 0 \quad (47)$$

in terms of a normalized diffusive flux defined as

$$F(S(x,t),x,t) = \frac{Q_{\mathbb{W}}(x,t) - Q(t)f_{\mathbb{W}}(S_r)}{Q_{\mathbb{W}}(0,t) - Q(t)f_{\mathbb{W}}(S_r)} \quad (48)$$

and the water flux

$$Q_{\mathbb{W}}(x,t) = Q(t)f_{\mathbb{W}}(S) - D(S) \frac{\partial S}{\partial x} \quad (49)$$

from Eq. (31). Passing to the similarity variable $\eta = x/\sqrt{t}$ in Eq. (47) gives for $t \neq 0$ and $0 < (dS/d\eta) < \infty$

$$\eta = \frac{2A[1 - f_{\mathbb{W}}(S_r)r] dF}{\phi \frac{dS}{d\eta}}, \quad (50)$$

while Eq. (48) becomes

$$F[S(\eta)] = \frac{rA[f_{\mathbb{W}}(S) - f_{\mathbb{W}}(S_r)] - D(S) \frac{dS}{d\eta}}{A - rAf_{\mathbb{W}}(S_r)}. \quad (51)$$

Here, by the same abuse of notation as for S , the same symbol F was used for two different functions. If $S(\eta)$ can be inverted, then Eq. (50) can be viewed as an equation for the inverse function $\eta(S)$. Taking the derivative d/dS on both sides of Eq. (50), inverting it, and inserting it for $dS/d\eta$ into Eq. (51) one arrives finally at the result

$$\frac{d^2 F}{dS^2} = -\frac{\phi}{2A^2[1 - f_{\mathbb{W}}(S_r)r]^2} \frac{D(S)}{F(S) - f(S)}, \quad (52)$$

where

$$f(S) = r \frac{f_{\mathbb{W}}(S) - f_{\mathbb{W}}(S_r)}{1 - rf_{\mathbb{W}}(S_r)} \quad (53)$$

was introduced as an abbreviation. Equation (52) is now interpreted not as an equation for the unknown function $S(\eta)$, but for the unknown function $F(S)$ with boundary conditions $F(S_r) = 0$, $F(S_\ell) = 1$, and $F'(S_\ell) = 0$ from Eq. (50). Its solution represents an implicit relation between the problem data.

The previous paragraph has shown that for similarity solutions with $\eta = x/\sqrt{t}$ an implicit relation exists between S_ℓ and A if S_r is considered to be fixed. While the problem formulation assumes that A is given and S_ℓ is to be found, it is numerically more convenient to exploit their relation with given S_ℓ and unknown A . An explicit equation for A is obtained by integrating Eq. (52) twice over the interval $[S_r, S_\ell]$ and using the boundary condition (33). It reads as

$$A^2 = \frac{\phi}{2[1 - rf_{\mathbb{W}}(S_r)]^2} \int_{S_r}^{S_\ell} \frac{(v - S_r)D(v)}{F(v) - f(v)} dv \quad (54)$$

and provides a one-to-one relation between A and S_ℓ . Integrating (52) twice and inserting (54) into the result yields an integral equation

$$F(S) = 1 - \frac{\int_S^{S_\ell} \frac{(v - S)D(v)}{F(v) - f(v)} dv}{\int_{S_r}^{S_\ell} \frac{(v - S_r)D(v)}{F(v) - f(v)} dv} \quad (55)$$

for F independent of A . Given the solution F , the saturation profile $S(\eta)$ is calculated from the inverse of (50). A numerical algorithm is required to determine the solution of Eq. (55), because its analytical solution is not known.

B. Numerical scheme

A simple iterative scheme for solving Eq. (55) is

$$F^{k+1}(S) = 1 - \frac{\int_S^{S_\ell} \frac{(v - S)D(v)}{F^k(v) - f(v)} dv}{\int_{S_r}^{S_\ell} \frac{(v - S_r)D(v)}{F^k(v) - f(v)} dv}. \quad (56)$$

Given the initial guess $F^{k=1}(S) = 1$ it converges rapidly in most cases but fails for $S_\ell \rightarrow 1 - S_{\text{Oim}}$. An iteration scheme which converges also for values S_ℓ closer to $1 - S_{\text{Oim}}$ was proposed by Fucik *et al.* [35]. Denoting the principal part of the integrals as $G = D/(F - f)$ it is written as

$$G^{k+1}(S) = D(S) + G^k(S) \left(f(S) - \frac{\int_S^{S_\ell} (v - S)G(v)dv}{\int_{S_r}^{S_\ell} (v - S_r)G(v)dv} \right). \quad (57)$$

The interval $[S_r, S_\ell]$ is discretized by N equidistantly distributed points. Hence, the i th saturation is $S_i = S_r + (i - 1)h$ with $h = (S_\ell - S_r)/(N - 1)$ and the i th element of G is defined as $G_i = G(S_r + (i - 1)h)$. The integrals in Eq. (57) are numerically approximated as

$$\begin{aligned} \mathcal{I}_j &:= \int_{S=S_r+(j-1)h}^{S_\ell} (v - S)G(v)dv \\ &= \sum_{i=j}^{N-1} \{a_i - [S_r + (j - 1)h]b_i\}, \end{aligned} \quad (58a)$$

$$\mathcal{I}_N := 0, \quad (58b)$$

where $j = 1, \dots, N - 1$ and the coefficients a_i, b_i stand for

$$\begin{aligned} a_i &= \int_{S_r+(i-1)h}^{S_r+ih} vG(v)dv \\ &\simeq \frac{h}{2} S_r (G_i + G_{i+1}) + \frac{h^2}{6} [(3i + 1)G_i + (3i + 2)G_{i+1}], \end{aligned} \quad (59a)$$

$$b_i = \int_{S_r+(i-1)h}^{S_r+ih} G(v)dv \simeq \frac{h}{2} (G_i + G_{i+1}), \quad (59b)$$

where $i = 1, \dots, N - 1$. With these definitions the iterative scheme reads as

$$G_j^{k+1} = D_j + G_j^k \left(f_j + \frac{\mathcal{I}_j}{\mathcal{I}_1} \right). \quad (60)$$

Note that \mathcal{I}_1 is the integral over the whole interval from S_r to S_ℓ . The flux coefficient A is calculated by inserting the discrete results into Eq. (54)

$$A = \sqrt{\frac{\phi \mathcal{I}_1}{2[1 - rf_{\mathbb{W}}(S_r)]^2}}. \quad (61)$$

As proposed by Fucik *et al.* [35], the iteration scheme is considered to be converged if

$$|A_{k+1} - A_k| < \epsilon, \quad (62)$$

where ϵ is the desired accuracy. The solution is

$$\eta(S_r + (j - 1)h) = \sqrt{\frac{2}{\phi \mathcal{L}_1}} \sum_{i=j}^{N-1} b_i. \quad (63)$$

It is obtained by integrating Eq. (52) only once and inserting the result together with Eqs. (59) and (61) into Eq. (50).

The numerical solutions obtained in this way may serve as a benchmark for direct numerical solvers of the original set of strongly coupled nonlinear partial differential equations.

C. Examples

For the computation of imbibition processes the fluid and rock properties are taken from [7]. They are listed in Table II. The viscous resistances are assumed to correspond to a permeability $k = 10^{-11} \text{ m}^2$, porosity $\phi = 0.347$, and viscosities $\mu_{\mathbb{W}} = 0.001 \text{ kg m}^{-1} \text{ s}^{-1}$ of water and $\mu_{\mathbb{O}} = 0.02 \text{ kg m}^{-1} \text{ s}^{-1}$ of oil. This results in resistance coefficients $R_{11} = 1.16 \times 10^6 \text{ kg m}^{-3} \text{ s}^{-1}$ and $R_{33} = 2.31 \times 10^7 \text{ kg m}^{-3} \text{ s}^{-1}$. The coefficient $R_{13} = 0 \text{ kg m}^{-3} \text{ s}^{-1}$ is assumed to vanish. The model parameters are summarized in Table II.

The simulations in this paper are restricted to imbibition processes. Drainage processes can be simulated similarly, but are not discussed due to space restrictions.

The parameters for the initial conditions and boundary conditions are specified in Table III. Initial conditions of type A correspond to a primary imbibition process, and initial conditions of type B to a secondary imbibition process. The initial conditions of type C correspond to a hypothetical experiment with a high fraction of nonpercolating phases.

Results for initial conditions A are shown in Fig. 3, for initial conditions B in Fig. 4, and a comparison for B and C is given in Fig. 5. For clarity the profiles are compared as functions of x at fixed time $t = 1000 \text{ s}$. All profiles are self-similar with respect to $\eta = x/\sqrt{t}$.

As $r \rightarrow 1$ and $S_{\ell} \rightarrow 1 - S_{\mathbb{O} \text{ im}}$ the required injected flux A increases and the flow is dominated by its advective hyperbolic part. Values for A for the different setups are given in Table III. Thus, diffusive second-order terms in saturations become less and less important. The theory for multiphase flow processes in porous media, which neglects diffusive saturation

TABLE III. Parameters for the initial and boundary values in Eqs. (34), (33), (36), and (37). The constant A is given in units of $10^{-3} \text{ m s}^{-1/2}$. It was chosen such that the saturation $S(0, t) = 0.7$ in all cases.

	A	B	C
$A(r = 0)$	0.312	0.283	0.258
$A(r = 0.8)$	0.560	0.571	0.554
$A(r = 1)$	3.797	4.550	4.774
S_r	0	0.15	0.15
S_{2r}	0	0.15	0.15
S_{4r}	0	0	0.19

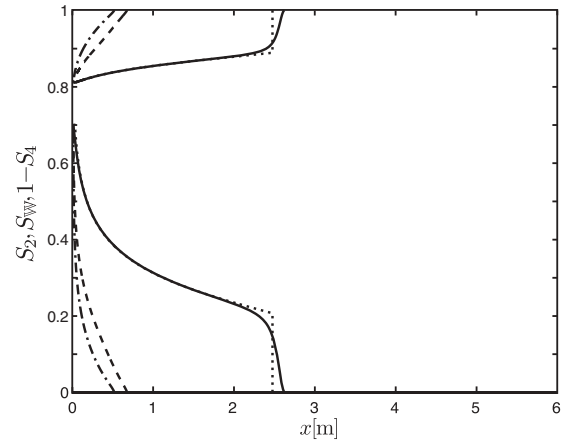


FIG. 3. Saturation profiles for primary imbibition processes (initial condition A) with three different values of r at $t = 1000 \text{ s}$. Solid curves correspond to $r = 1$, dashed curves to $r = 0.8$, and dash-dotted curves to $r = 0$. The saturation profiles of the Buckley-Leverett problem with flux decreasing as $\sim 1/\sqrt{t}$ are shown for comparison as dotted curves. The profile $S_2 = 0$ coincides with the x axis. The profile $S_{\mathbb{W}}$ has values in the saturation range from 0 to 0.7, and the profile $1 - S_4$ has values in the range from 0.8 to 1.

terms of second order in space, is commonly known as the Buckley-Leverett theory. It was recently adapted to account for immobile nonpercolating fluid parts [30]. The solutions of the Buckley-Leverett theory for initial conditions with a single discontinuity in space are self-similar with x/t for constant total flux Q . If the flux is decreased as $Q \propto 1/\sqrt{t}$ the solutions are self-similar with $\eta = x/\sqrt{t}$ and a comparison of the solutions of both considered methods is feasible. Although the solutions for $r = 0.8$ and $r = 0$ show the same self-similarity, a comparison is omitted due to the absence of fronts in these profiles.

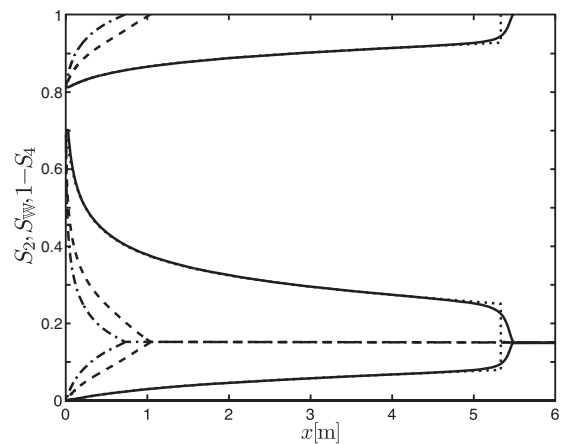


FIG. 4. Saturation profiles for secondary imbibition processes (initial condition B) with three different values of r at $t = 1000 \text{ s}$. Solid curves correspond to $r = 1$, dashed curves to $r = 0.8$, and dash-dotted curves to $r = 0$. The saturation profiles of the Buckley-Leverett problem with flux decreasing as $\sim t^{-1/2}$ are shown for comparison as dotted curves. The profile S_2 has values in the range from 0 to 0.15. The profile $S_{\mathbb{W}}$ has values in the saturation range from 0.15 to 0.7, and the profile $1 - S_4$ has values in the range from 0.81 to 1.

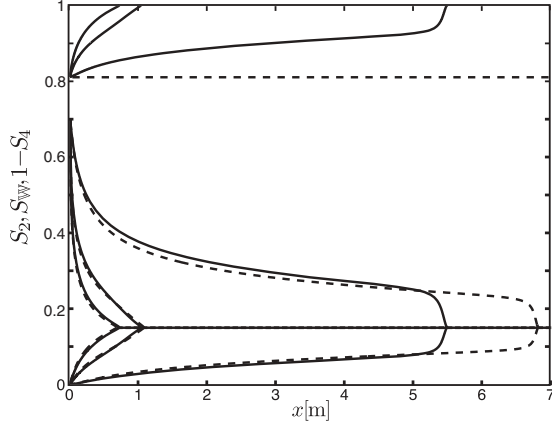


FIG. 5. Comparison of saturation profiles for initial conditions B and C with three different values of $r = 0$ (left profiles), $r = 0.8$ (middle profiles), and $r = 1.0$ (right profiles) at $t = 1000$ s. Solid curves correspond to initial conditions of type B and dashed curves to initial conditions of type C. The profiles S_2 have values in the range from 0 to 0.15. The profiles S_{ww} have values in the saturation range from 0.15 to 0.7, and the profiles $1 - S_4$ have values in the range from 0.81 to 1.

Figure 3 shows saturation profiles for different values of r with respect to the spatial coordinate x at time $t = 1000$ s. All cases show a displacement of oil by water. As the percolating oil is displaced, nonpercolating oil is produced by breakup. The invasion front has reached a five times larger distance from the injection well if the porous medium permits full outflow at the right boundary ($r = 1$) compared to impeded outflow ($r = 0, 0.8$). If outflow at the right side is impeded, the diffusive contribution is dominating the process. Compared to linear diffusion the propagation is suppressed for low saturations because $D(S) \rightarrow 0$ for $S \rightarrow 0$ as illustrated in Fig. 2. For $r = 1$ the advective part is dominant and the profile is close to a rarefaction shock as expected from Buckley-Leverett theory. A comparison of the Buckley-Leverett solution and the solution for $r = 1$ shows that both predict the same velocity of the shock. For higher saturations $S_\ell \rightarrow 1 - S_{\text{Oim}}$ the diffusive similarity solution approaches the Buckley-Leverett solution even closer.

Figure 4 shows saturation profiles similar to Fig. 3 but for a secondary imbibition. Qualitatively the results are similar to the primary imbibition solutions. Advection dominates the solution for $r = 1$ and diffusion for $r = 0$ and 0.8.

A comparison of the solution for primary (Fig. 3) and secondary (Fig. 4) imbibition yields two remarkable insights. A significantly higher water injection rate is required for the secondary imbibition to maintain a constant saturation $S = 0.7$ at the inlet compared to the primary imbibition. This is explained by the increase of the mobility of the water due to coalescence of nonpercolating water with the percolating water. The effect is pronounced for $r = 1$ and $r = 0.8$. It is absent for $r = 0$. Such an effect is not predicted by the traditional theory, where the saturations are rescaled using effective saturations instead of real saturations. To capture this effect within the traditional theory different sets of constitutive parameters would have to be applied for primary and secondary

imbibition processes, while the present approach uses a single parameter set for all processes.

Figure 5 shows a comparison of saturation profiles for initial conditions of types B and C. Solid curves correspond to initial conditions B and dashed curves correspond to initial conditions C. As before, saturation profiles are shown for the values $r = 0, 0.8, 1.0$. Qualitatively the solutions for both initial conditions (B and C) are similar. Quantitatively, only the case $r = 1.0$ (free outflow, advection dominated) shows a significant difference: the invasion front is faster if more nonpercolating oil is initially present in the medium. The mathematical reason for this behavior is that the fractional flow function $f_{\text{ww}}(S)$ in Eq. (43) has for $S < 0.25$ a higher slope for initial condition C than for B. As a consequence the derivative df/dS is much higher in this saturation range and this term dominates over the diffusive term in Eq. (43) when $r \rightarrow 1$. Physically this reflects the fact that the presence of nonpercolating oil reduces the volume available to water in cocurrent flow ($r = 1$) so that at comparable flow rates (cf. Table III) the front velocity must be increased.

Figures 3–5 all show that the different hydrodynamic properties of percolating and non-percolating phases might lead to effects that could be measured in laboratory experiments. In particular, the effects of initial nonpercolating water on the imbibition process are not predicted by the traditional theory. The effects predicted here could hardly be included in the traditional theory, because every initial condition would require a reparametrization of all parameter functions of the traditional theory.

VIII. CAPILLARITY-DRIVEN HORIZONTAL REDISTRIBUTION [32]

A. General solution

The method of solution of the capillarity-driven horizontal distribution problem at zero flux parallels the treatment of [32]. Our presentation follows closely that of [37].

The initial conditions (36) are homogeneous with one discontinuity at $x = 0$. Without loss of generality $S_r < S_\ell$ is assumed. For a water wet medium, capillary forces will then drive the water from the left into the right domain and oil from right to left, because there is no net flux. By inserting Eq. (35) into Eq. (43), the initial and boundary value problem is subdivided into

$$\phi \frac{\partial S}{\partial t} - \frac{\partial}{\partial x} \left(D^\ell(S) \frac{\partial S}{\partial x} \right) = 0, \quad (64a)$$

$$S(x, 0) = S_\ell, \quad S(-\infty, t) = S_\ell \quad (64b)$$

for $x < 0$, and

$$\phi \frac{\partial S}{\partial t} - \frac{\partial}{\partial x} \left(D^r(S) \frac{\partial S}{\partial x} \right) = 0, \quad (65a)$$

$$S(x, 0) = S_r, \quad S(\infty, t) = S_r \quad (65b)$$

for $x > 0$. We introduce here the notation

$$\mathcal{F}^j(S) = \mathcal{F}(S, S_2(S; S_i, S_{2i}), S_4(S; S_i, S_{4i})), \quad (66)$$

where $j = \ell, r$ and $\mathcal{F} = D, \lambda, P_c$ to distinguish left and right parameter functions. The macroscopic capillary diffusion coefficients D^ℓ, D^r , the fractional mobilities λ^ℓ, λ^r , and the

capillary pressure functions P_c^ℓ, P_c^r differ in the left and right domains because of the initial conditions. The initial and boundary value problems (64) and (65) are not closed. Physical considerations [32,37] require that pressures and fluxes at the interface between the two domains at $x = 0$ are continuous. This reads as

$$\lim_{x \nearrow 0} Q_{\mathbb{W}}(x, t) = \lim_{x \searrow 0} Q_{\mathbb{W}}(x, t), \quad (67a)$$

$$\lim_{x \nearrow 0} P_c^\ell(S(x, t)) = \lim_{x \searrow 0} P_c^r(S(x, t)). \quad (67b)$$

Hence, the solution strategy is to find self-similar solutions of the two initial and boundary value problems (64) and (65) in the similarity variable $\eta = x/\sqrt{t}$. This results in two boundary value problems:

$$\frac{\phi}{2} \eta S' + [D^\ell(S)S']' = 0, \quad (68a)$$

$$S(-\infty) = S_\ell, \quad (68b)$$

$$S(0-) = S_-, \quad (68c)$$

for $\eta \in (-\infty, 0)$, and

$$\frac{\phi}{2} \eta S' + [D^r(S)S']' = 0, \quad (69a)$$

$$S(+\infty) = S_r, \quad (69b)$$

$$S(0+) = S_+, \quad (69c)$$

for $\eta \in (0, +\infty)$. Here a prime ' denotes the derivative $d/d\eta$. The boundary values S_-, S_+ remain to be specified. The physical constraints (67) are now applied to specify them.

Whenever the capillary functions P_c^ℓ, P_c^r defined in Eq. (66) are invertible it is possible to define the two functions $h_+^\pm(s), h_-^\pm(s) : [0, 1] \rightarrow [0, 1]$ by

$$h_+^\pm(s) := (P_c^r)^{-1} \circ (P_c^\ell(s)), \quad (70a)$$

$$h_-^\pm(s) := (P_c^\ell)^{-1} \circ (P_c^r(s)), \quad (70b)$$

where $(P_c^i)^{-1}$ with $i = \ell, r$ denotes the inverse of the corresponding capillary function. With the help of these functions the constraint on the pressures (67b) reads as

$$S_+ = h_+^-(S_-), \quad (71a)$$

$$S_- = h_-^+(S_+). \quad (71b)$$

The continuity condition for the fluxes (67a) is now applied to obtain a second constraint. It has been shown [38] that for every saturation $S_- < S_\ell$ the boundary value problem (68) has a unique decreasing solution. Similarly, for every saturation $S_+ > S_r$ the boundary value problem (69) has a unique increasing solution. With these solutions the ‘‘quasi-fluxes’’

$$\tilde{Q}_-(S_-) = \lim_{\eta \nearrow 0} D^\ell(S) \frac{dS}{d\eta}, \quad (72a)$$

$$\tilde{Q}_+(S_+) = \lim_{\eta \searrow 0} D^r(S) \frac{dS}{d\eta} \quad (72b)$$

at the origin are given as functions of the saturations at the boundary. The term ‘‘quasi-flux’’ is used because they have to be divided by \sqrt{t} to obtain physical fluxes. It has further been shown [38] that if $S_- > h_+^-(S_r)$ holds, $\tilde{Q}_-(S_-)$ is continuously decreasing with respect to $S_- \in [h_+^-(S_r), S_\ell]$. It is vanishing

at its maximum saturation $\tilde{Q}_-(S_\ell) = 0$ and hence $\tilde{Q}_-(S_-) > 0$ for $S_- \in [h_+^-(S_r), S_\ell]$. Similarly, if $S_r < h_-^+(S_\ell)$ holds, $\tilde{Q}_+(S_+)$ is a continuously increasing function with respect to $S_+ \in [S_r, h_-^+(S_\ell)]$. It is vanishing at its minimum saturation $\tilde{Q}_+(S_r) = 0$ and hence $\tilde{Q}_+(S_+) > 0$ for $S_+ \in [S_r, h_-^+(S_\ell)]$. At this point we note an error in Theorem 2 on page 387 of [37]. The words ‘‘decreasing’’ and ‘‘increasing’’ have to be exchanged. The same error appeared again in the discussion on page 135 of [39].

From the properties of \tilde{Q}_-, \tilde{Q}_+ it is concluded that if there is a solution pair (S_-, S_+) with $\tilde{Q}_-(S_-) = \tilde{Q}_+(S_+)$, then it is unique. Continuity of fluxes and pressures makes the solution unique. Expressing the saturation S_+ in \tilde{Q}_+ in terms of S_- with function (70b) one defines a function for the difference of the quasi-fluxes at the origin $\Delta \tilde{Q}(s) = \tilde{Q}_-(s) - \tilde{Q}_+(h_+^-(s))$ which is a continuous and monotonically decreasing function with $\Delta \tilde{Q}(h_+^-(S_r)) > 0$ and $\Delta \tilde{Q}(S_\ell) < 0$. Therefore $\Delta \tilde{Q}$ has a unique root in $[h_+^-(S_r), S_\ell]$ and the problem is well posed. However, there is no simple expression for the fluxes available and an iterative procedure for solving the boundary value problems (68) and (69) is required. In the remainder of this section the boundary value problems (68) and (69) are transformed as in Ref. [37]. This transformation permits a more effective algorithm, because it directly solves for the quasi-fluxes and computes the saturation profile only once at the end.

The monotonicity of S in $\eta \in (\eta_\ell, 0)$, where $\eta_\ell = \max\{\eta | S(\eta) = S_\ell\}$, permits a transformation of the ordinary differential equation (68) for $S = S(\eta)$ into an ordinary differential equation for $\eta = \eta(S)$. With $S'(\eta) = 1/\eta'(S)$ and $\tilde{Q}_\ell(S) = D^\ell(S)(dS/d\eta)$ the result of the transformation reads as

$$\frac{\partial}{\partial S} \tilde{Q}_\ell(S) = \frac{\phi}{2} \eta \quad \text{for } S_- < S < S_\ell. \quad (73)$$

By taking the derivative with respect to S and inserting $\eta' = -D/\tilde{Q}_\ell$ one obtains an ordinary differential equation for $\tilde{Q}_\ell(S)$ which is independent of η . For $\eta > 0$ the procedure is completely analogous and finally the two boundary value problems

$$\tilde{Q}_\ell(S) \frac{d^2}{dS^2} \tilde{Q}_\ell(S) = -\frac{\phi}{2} D^\ell(S), \quad (74a)$$

$$\frac{d}{dS} \tilde{Q}_\ell(S_-) = 0, \quad \tilde{Q}_\ell(S_\ell) = 0, \quad (74b)$$

for $S_- < S < S_\ell$, and

$$\tilde{Q}_r(S) \frac{d^2}{dS^2} \tilde{Q}_r(S) = -\frac{\phi}{2} D^r(S), \quad (75a)$$

$$\frac{d}{dS} \tilde{Q}_r(S_+) = 0, \quad \tilde{Q}_r(S_r) = 0, \quad (75b)$$

for $S_r < S < S_+$, have to be solved. The boundaries S_-, S_+ remain part of the solution due to the continuity of pressures and fluxes and an iterative procedure is required. Given $\tilde{Q}_\ell(S), \tilde{Q}_r(S)$, the inverse of the saturation profile with Eq. (73) and the right-side equivalent is

$$\eta(S) = \begin{cases} \frac{2}{\phi} \frac{d}{dS} \tilde{Q}_r(S), & \text{for } S_r < S < S_+, \\ \frac{2}{\phi} \frac{d}{dS} \tilde{Q}_\ell(S), & \text{for } S_- < S < S_\ell. \end{cases} \quad (76)$$

Taken together, this defines the following algorithm.

TABLE IV. Initial conditions for the capillarity-driven horizontal redistribution problem.

	D	E
S_r	0	$S_{\text{W dr}}$
S_{2r}	0	$S_{\text{W dr}}$
S_{4r}	0	0
S_ℓ	1	$1 - S_{\text{O im}}$
$S_{2\ell}$	0	0
$S_{4\ell}$	0	$S_{\text{O im}}$

Pseudocode for calculating $S(\eta)$

- Determine $S_< := h_-(S_r)$ and $S_> := S_\ell$
 - while $S_> - S_< > \epsilon$ do
 - $S_- = (S_> + S_<)/2$
 - Solve (74) to find the quasi-flux $\tilde{Q}_\ell(S_-)$
 - $S_+ = h_+(S_-)$
 - Solve (75) to find the quasi-flux $\tilde{Q}_r(S_+)$
 - if $\tilde{Q}_\ell(S_-) - \tilde{Q}_r(h_+(S_-)) > 0$: $S_< = S_-$
 - if $\tilde{Q}_\ell(S_-) - \tilde{Q}_r(h_+(S_-)) < 0$: $S_> = S_-$
 - obtain $S(\eta)$ by inverting (76)
- Here ϵ denotes the desired accuracy.

B. Implementation

Our solution algorithm goes beyond [37] or [32] in two respects. First, the capillary pressure is an algebraic equation instead of an ordinary differential equation in Ref. [37] and invertible by principle. The relatively cumbersome algebraic inversion is avoided by inverting an arbitrary, precisely fitted, piecewisely interpolated polynomial numerically. Second, an implicit finite-difference method in conjunction with a Newton-Raphson method is used here to solve the boundary value problems in Eqs. (74) and (75). The implementation requires more effort than the originally used shooting technique [37] but it is compensated by a substantially quicker convergence. Further it directly ensures the Neumann

 TABLE V. Saturations at $x = 0^-$ and $x = 0^+$ for the primary and secondary redistribution.

	Primary		Secondary	
	-	+	-	+
S	0.506	0.161	0.438	0.281
S_2	0.145	0	0.145	0.062
S_4	0	0.092	0.016	0.092

boundary condition at S_-, S_+ by considering them explicitly in the discretization scheme.

C. Examples

For calculating saturation profiles the parameters from Table II are used. Redistribution profiles are shown for the two different initial conditions listed in Table IV. Initial conditions of type D correspond to a primary redistribution, and initial conditions of type E correspond to a secondary redistribution. A primary redistribution consists of a primary drainage in the right and a primary imbibition in the left domain. A secondary redistribution consists of a secondary drainage in the right and a secondary imbibition in the left domain. For clarity the profiles are plotted with respect to space x at time $t = 1000$ s although the profiles are self-similar with respect to $\eta = x/\sqrt{t}$. Characteristic values of the solutions are listed in Table V.

Figure 6(a) shows saturation profiles for the primary redistribution. The initial conditions are depicted as dashed lines and profiles at $t = 1000$ s as solid curves. The water is soaked into the right domain through capillary forces. The displacement of the oil leads to a production of nonpercolating oil in the right domain. The oil invades the left domain and water eventually breaks up while its saturation is decreasing and nonpercolating water is produced. A discontinuity in the saturation remains at $x = 0$ for all times. Nonpercolating water in the right domain and nonpercolating oil in the left domain are not produced.

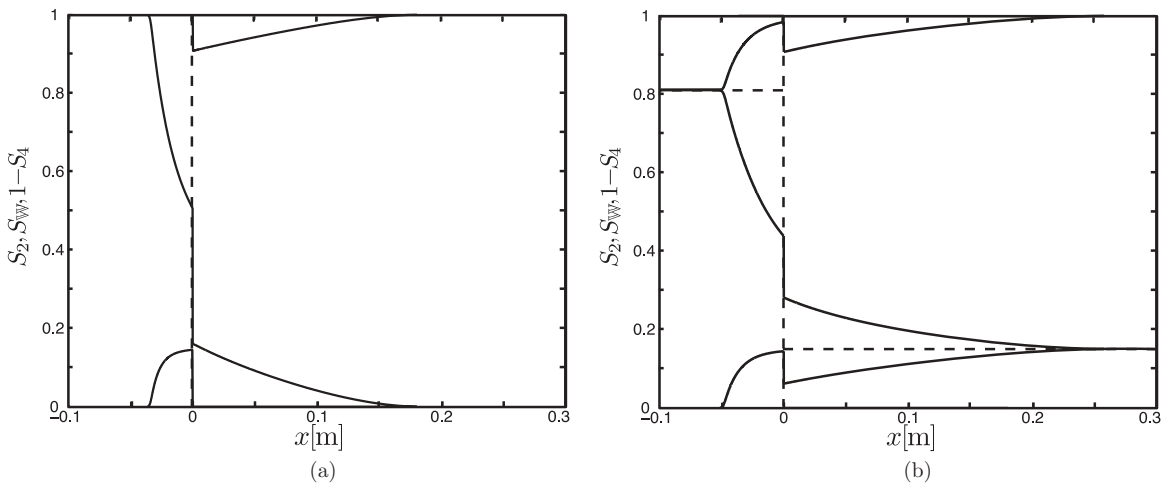


FIG. 6. Saturation profiles for the Philip problem for (a) a primary redistribution and (b) a secondary redistribution. Solid curves show profiles at $t = 1000$ s and dashed lines show the initial conditions. Profile S_2 has values in the range from 0 to 0.15. Profile S_{W} has values in the saturation range from 0.15 to 0.7, and profile $1 - S_4$ has values in the range from 0.81 to 1.

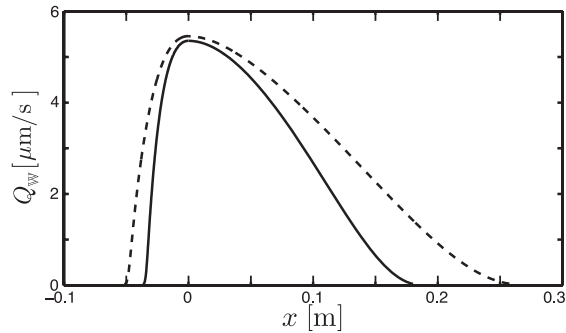


FIG. 7. Flux profiles at $t = 1000$ s for the Philip problem. The solid curve corresponds to a primary redistribution and the dashed curve to a secondary redistribution.

Figure 6(b) shows saturation profiles for the secondary redistribution. The initial conditions are depicted as dashed lines and profiles at $t = 1000$ s as solid curves. The water is soaked into the right domain through capillary forces. The displacement of the oil there leads to a production of nonpercolating oil and a reduction to nonpercolating water in the right domain. The invasion of the oil into the left domain produces nonpercolating water and reduces nonpercolating oil. Again a discontinuity remains forever at $x = 0$.

A comparison of primary and secondary processes shows that the speed of the redistribution is not substantially altered by the presence of the nonpercolating fluids. But, as for horizontal flows discussed above, the redistribution is facilitated by the presence of nonpercolating fluids. The height of the saturation jump at $x = 0$ differs significantly for both processes.

Figure 7 shows flux profiles for both redistribution problems. The flux is maximal at the discontinuity and vanishes for $|x| \rightarrow \infty$. The flux for the primary redistribution is shown as a solid curve and for the secondary redistribution as a dashed curve. It is seen in this figure that the redistribution for the secondary processes is slightly faster. Fluxes are everywhere larger than for the primary processes.

These results show that the theory presented here allows one to model different processes by a single set of parameters without advance knowledge of the type of process. The theory discussed here predicts a permanent discontinuity in saturation at the boundary regions of differing process history, and it

identifies the differences in nonpercolating fluid phases as the origin of this discontinuity. Contrary to this, the traditional theory requires advance knowledge of the processes that will occur in a region. Discontinuities in the parametrization within the traditional theory then allow one to model the phenomenon but do not provide a physical explanation for it.

IX. CONCLUSION

A limit for a recent mathematical model for multiphase flow in porous media was obtained by considering a one-dimensional homogeneous porous medium and assuming that nonpercolating fluid phases are immobile. The assumptions permit one to transform the original ten coupled nonlinear partial differential equations to only three partial differential equations. Two of these are integrated analytically and the remaining partial differential equation was solved for two initial and boundary value problems, commonly known as the McWhorter-Sunada problem and the Philip redistribution problem. The remaining partial differential equation was transformed into an ordinary differential equation which was solved numerically by iterative procedures introduced by Fucik *et al.* [35] for the McWhorter-Sunada problem and by Pop *et al.* [37] for the Philip problem. The solutions of the McWhorter-Sunada problem show that taking into account nonpercolating phases has a significant impact on the required injected flux rate and the velocity of the advancing front. They show also that solutions of the hyperbolic limiting case found recently in Ref. [30] coincide with the vanishing capillarity approach. The solutions of the Philip problem illustrate the capability of mapping the whole hysteresis cycle with one set of parameters if differences in percolating and nonpercolating fluid regions are taken into account properly. It further shows that a discontinuity in water saturation may be stationary even in a homogeneous medium.

ACKNOWLEDGMENTS

The authors acknowledge Dr. I. S. Pop for a helpful discussion. They are grateful to the Deutsche Forschungsgemeinschaft through its International Research and Training Group (IRTG) on Nonlinearities and Upscaling in Porous Media (NUPUS) for financial support.

-
- [1] R. Hilfer, *Adv. Chem. Phys.* **92**, 299 (1996).
 - [2] M. Muskat, *The Flow of Homogeneous Fluids through Porous Media* (McGraw-Hill, New York, 1937).
 - [3] R. Collins, *Flow of Fluids through Porous Materials* (Reinhold, New York, 1961).
 - [4] D. Stauffer and A. Aharony, *Introduction to Percolation Theory* (Taylor and Francis, London, 1992).
 - [5] M. Sahimi, *Flow and Transport in Porous Media and Fractured Rock* (Wiley-VCH Verlag, Weinheim, Germany, 1995).
 - [6] R. Hilfer, *Phys. Rev. E* **73**, 016307 (2006).
 - [7] R. Hilfer, *Physica A* **371**, 209 (2006).
 - [8] R. Wyckoff and H. Botset, *Physics* **7**, 325 (1936).
 - [9] A. Scheidegger, *The Physics of Flow Through Porous Media* (University of Toronto, Toronto, 1974).
 - [10] K. Aziz and A. Settari, *Petroleum Reservoir Simulation* (Applied Science, London, 1979).
 - [11] M. Honarpour, L. Koederitz, and A. Harvey, *Relative Permeability of Petroleum Reservoirs* (CRC, Boca Raton, FL, 1986).
 - [12] A. Poulouvasilis and E. Childs, *J. Soil Sci.* **112**, 301 (1971).
 - [13] Y. Mualem, *Water Resour. Res.* **10**, 514 (1974).
 - [14] J. Parker and R. Lenhard, *Water Resour. Res.* **23**, 2187 (1987).
 - [15] G. Barenblatt, V. Entov, and V. Ryzhik, *Theory of Fluid Flows Through Natural Rocks* (Kluwer, New York, 1990).

- [16] S. Hassanizadeh and W. G. Gray, *Water Resour. Res.* **29**, 3389 (1993).
- [17] S. Hassanizadeh, M. Celia, and H. Dahle, *Vadose Zone J.* **1**, 38 (2002).
- [18] S. Manthey, M. Hassanizadeh, R. Helmig, and R. Hilfer, *Adv. Water Res.* **31**, 1137 (2008).
- [19] A. Abrams, *Soc. Pet. Eng. J.* **15**, 437 (1975).
- [20] D. G. Avraam and A. C. Payatakes, *Transp. Porous Media* **20**, 135 (1995).
- [21] D. G. Avraam and A. C. Payatakes, *J. Fluid Mech.* **293**, 207 (1995).
- [22] J. Taber, *Soc. Pet. Eng. J.* **9**, 3 (1969).
- [23] R. Hilfer, *Phys. Rev. E* **58**, 2090 (1998).
- [24] R. Hilfer and H. Besserer, in *Porous Media: Physics, Models, Simulation*, edited by A. Dmitrievsky and M. Panfilov (World Scientific, Singapore, 2000), p. 133.
- [25] R. Hilfer and H. Besserer, *Physica B* **279**, 125 (2000).
- [26] R. Hilfer, *Physica A* **359**, 119 (2006).
- [27] R. Hilfer, in *CP1091, Modeling and Simulation of Materials*, edited by P. Garrido, P. Hurtado, and J. Marro (American Institute of Physics, New York, 2009), p. 141.
- [28] R. Hilfer and F. Doster, *Transp. Porous Media* **82**, 507 (2010).
- [29] F. Doster, P. A. Zegeling, and R. Hilfer, *Phys. Rev. E* **81**, 036307 (2010).
- [30] F. Doster and R. Hilfer, *New J. Phys.* **13**, 123030 (2011).
- [31] D. McWhorter and D. Sunada, *Water Resour. Res.* **26**, 399 (1990).
- [32] J. Philip, *Water Resour. Res.* **27**, 1459 (1991).
- [33] R. Hilfer and P. Øren, *Transp. Porous Media* **22**, 53 (1996).
- [34] D. McWhorter and D. Sunada, *Water Resour. Res.* **28**, 1479 (1992).
- [35] R. Fucik, J. Mikyuska, M. Benes, and T. Illangasekare, *Vadose Zone J.* **6**, 93 (2007).
- [36] By an abuse of notation the same symbol S is used for $S(x,t)$ and $S(\eta)$ although the two functions are different. This should not cause any confusion, because which function is meant is clear from the number of arguments.
- [37] I. Pop, C. Duijn, J. Niessner, and M. Hassanizadeh, *Adv. Water Resour.* **32**, 383 (2009).
- [38] C. Duijn and M. Neef, *Adv. Water Resour.* **21**, 451 (1998).
- [39] F. Doster, Ph.D. thesis, University of Stuttgart, 2011.